Indonesian Journal of Electrical Engineering and Informatics (IJEEI)
Vol. 10, No. 3, September 2022, pp. 655~667
ISSN: 2089-3272, DOI: 10.52549/ijeei.v10i3.3895

A Robust Controller Design for Simple Robotic Human Arm

Wajdi Sadik Aboud[1], Hadeel K. Aljobouri[2], Hayder Sabah Abd Al-Amir[3]
[1]Prosthetics and Orthotics Engineering Department, College of Engineering, Al-Nahrain University, Baghdad, Iraq
[2]Biomedical Engineering Department, College of Engineering, Al-Nahrain University, Baghdad, Iraq
[3]Power Mechanics Department, Institute of Technology – Baghdad, Middle Technical University, Baghdad, Iraq

Article Info

Article history:

Received May 22, 2022
Revised Sep 6, 2022
Accepted Sep 17, 2022

Keyword:

Adaptive,
Manipulator,
Robotic arm,
Sliding mode control (SMC),
Trajectory tracking

ABSTRACT

Nowadays, the manipulator of two degrees of freedom (2DOF) has many applications. One is a human arm that may be utilized in robotic rehabilitation. The 2DOF controlled robot manipulator usually acts like human arms. This paper aims to design a robust, stable controller for the upper limb robotic model. A sliding mode control (SMC) approach is proposed to realize stability, tracing accuracy, and robustness for 2DOF robotic manipulator. Based on the general manipulator equation of motion, two SMCs are designed. The first is designed according to the input–output stability constraints. The second is designed according to the adaptive law. Not only the trajectory tracking is guaranteed but also stability is ensured. The stability of the controllers is examined based on Lyapunov stability criteria. The controllers and the robotic arm are formulated analytically. The MATLAB platform is adopted to examine and validate the proposed controller's performance. The addition of adaptation law in the SMC scheme improves the results for the two designed controllers and shows remarkable trajectory tracking and system stability as well. The improvement rate shows an enhancement of 40.5% and 36.7% for manipulator joints 1 and 2, respectively.

Corresponding Author:

Wajdi Sadik Aboud
Prosthetics and Orthotics Engineering Department,
College of Engineering, Al-Nahrain University,
Baghdad 10072, IRAQ
Email: wajdisadik@gmail.com

1. INTRODUCTION

Recently, robots are commonly utilized to perform variant jobs rapidly with a high degree of accuracy and reliability compared with that done by humans. The arm of a human has seven degrees of freedom (DOF), but simplifying by adopting initially two degrees of freedom (2DOF) robot manipulator is the easier task to understand the complexity of the human arm. In addition, the controlling process and the control type are crucial tasks to achieve the required desired performances [1].

Nowadays, robotic rehabilitation is a new field that is immensely developing. It consists of the enhancement of robotic therapies by adopting robots as therapy aids instead of using the robots as assistive devices by therapists [2]. Studies verified that the existence of robots through rehabilitation becomes a strong factor to improve the movement ability of patients when they suffer from impairments either due to orthopedic or neurological diseases. The improvement of the muscle strength and movement coordination of these patients according to the automated robot-assisted, task-oriented repetitive movements is also verified [3, 4]. Thus, the problem of designing an appropriate controller for a robotic manipulator that demands low errors and high stability is still open. Several attempts have been made to focus on the design of the articulated two-link robotic manipulator system for either a linear or a nonlinear controller based on classical as well as modern controllers or both.

An intelligent controller was constructed for a two-link robot manipulator based on a fuzzy system [5, 6]. PID has been used for different for medical applications [7–9]. In 2020, Baccouch et al. proposed a robust, fast PID controller for the classical double pendulum system [10]. In 2021, The trajectory tracking control of a two-link planar robot manipulator was considered using the PID and sliding mode control (SMC) controller by Ilgen et al. [11]. Mathew & Rikesh proposed strategy using the PID and SMC for controlling the position of end effector [12]. In 2017, Zulfatman et al. proposed using SMC with linear matrix inequality for moderating the properties of chattering on the sliding surface [13].

Usually, some differences appear when creating a mathematical model to represent real plants in controller design processes because of many different valued factors. Despite these differences, engineers have to provide suitable levels of the required performance. In recent times, a great development was observed in the types of controllers, especially those that are based on adaptation techniques and deal with nonlinear systems. Non-linear systems with disturbances and parameter uncertainties are controlled by using the developed controllers such as multiple models adaptive, intelligent adaptive models, and composite adaptive techniques [14, 15]. In 2016, multiple model adaptive PID controllers were proposed for four operating mode conditions. They were subjected to a nonlinear mechatronic suspension [16]. In 2020, Liu et al. presented a mechanical adaptive control method based on an intelligent neural network model based on the radial basis function neural network model for a multiDOF manipulator [17].

In addition, many robust control approaches were developed to reduce and eliminate any of these differences. One such method is the SMC methodology used for robust control design. It is a particular kind of variable structure control system. SMC was utilized in a broad method of design being tested for a wide variety of system types including, multi-input multioutput (MIMO) systems, nonlinear systems, stochastic systems, and time-varying systems. The furthermost notable feature of SMC is that is not affected by external disturbances and parametric uncertainty throughout the sliding mode [18, 19] In 2021, Kumar et al. designed an SMC for frequency regulation in an interconnected power system. They selected four parameters for the load frequency control (LFC) system model. These parameters were obtained by particle swarm optimization (PSO) and grey wolf optimization (GWO) approaches [20]. Based on a finite time SMC strategy, Wang et al. proposed a robust, adaptive SMC subject to control input limitations for both MIMO and single-input single-output (SISO) systems [21].

On the one hand, robotic manipulators are generally subjected to uncertainties according to the weight of links and payload variations [22]. On the other hand, robotic manipulators are known as dynamically coupled, time-varying, and highly nonlinear systems that are utilized broadly in medical applications nowadays. Owing to these uncertainties and nonlinear behavior, controlling the motion of the robot manipulator at an accurate position is a challenging task. For precise applications, any robot should follow the desired trajectories with minimal errors as much as possible. The trajectory tracking control task is a very necessary, essential requirement in controlling manipulators [19].

Therefore, the current paper focuses on the design of a controller for a 2DOF robotic manipulator that demands low effort with low error as well as stability guarantees. The main aim of this paper is to design appropriate controllers represented by SMCs for a robot manipulator of 2DOF that is fast for trajectory tracking and effective when disturbances and uncertainties are found.

2. ROBOT ARM MODELING

The modeling of the proposed 2DOF robot arm is presented in the following two paragraphs.

2.1. General Modeling

Manipulators are the familiar system models in robotics. The general considering equation of motion for *n*-joint robot manipulator is given by [23, 24]:

$$\boldsymbol{H}(\boldsymbol{q})\ddot{\boldsymbol{q}} + \boldsymbol{C}(\boldsymbol{q},\dot{\boldsymbol{q}})\dot{\boldsymbol{q}} + \boldsymbol{G}(\boldsymbol{q}) + \boldsymbol{F}(\dot{\boldsymbol{q}}) + \boldsymbol{\tau_d} = \boldsymbol{\tau}, \tag{1}$$

where $\boldsymbol{q}$ is the generalized coordinate (the angle vector), and $\boldsymbol{q} \in \boldsymbol{R^n}$; $\boldsymbol{H(q)}$ is the inertia matrix, and $\boldsymbol{H(q)} \in \boldsymbol{R^{n\times n}}$; $\boldsymbol{C(q,\dot{q})}$ represents the centrifugal and the Coriolis forces, and $\boldsymbol{C(q,\ \dot{q})} \in \boldsymbol{R^n}$; $\mathrm{G}(\boldsymbol{q}) \in \boldsymbol{R^n}$ and $\boldsymbol{F(\dot{q})} \in \boldsymbol{R^n}$ $\boldsymbol{I}$ are the gravity and the frictional force, respectively; $\boldsymbol{\tau}$ denotes the control moment, and $\boldsymbol{\tau} \in \boldsymbol{R^n}$; $\boldsymbol{\tau_d}$ represents the disturbance moment, and $\boldsymbol{\tau_d} \in \boldsymbol{R^n}$.

By assuming that the kinetic model of a manipulator has the following characteristics [25],

i. The kinetic model has many items, which are increased when the number of robot joints is increased.
ii. Parameter nonlinearity: Each parameter of the equations has nonlinearity represented, for example, by trigonometric functions.
iii. Coupling has a high degree.
iv. Uncertainty is represented by an inconstant load.
v. The time-variant model is represented by the friction torque in joints that changes with time.
vi. Inertia matrix $H(q)$ is bounded and positive-definite symmetrical.
vii. $C(q,\dot{q})$ is bounded, which means $c_b(q)$ if $|C(q,\dot{q})| \leq\ c_b(q)||\dot{q}||$.

viii. Matrix $\dot{H} - 2C$ is a skew-symmetric matrix.
ix. Disturbance τ_d agrees with $||\tau_d|| \le \tau_M$, where τ_M is a positive constant.

Figure 1 illustrates the conventional dual-joint rigid manipulator including the main parameters.

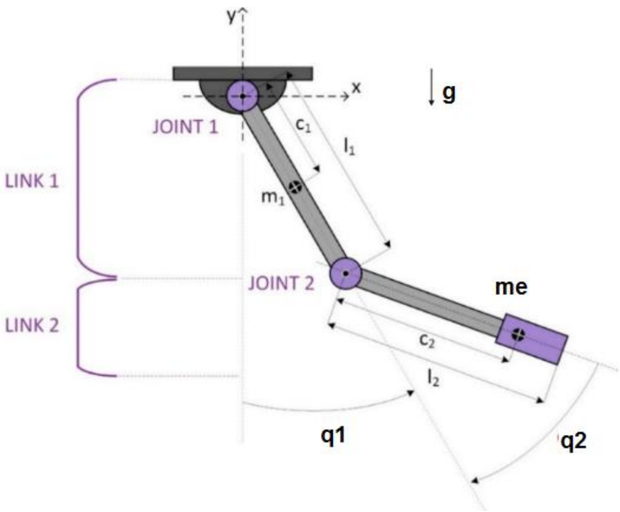

Figure 1. Physical structure of a dual-joint manipulator includes load [26]

2.2. Modeling of 2DOF Robot Arm

The dynamic equation for the 2DOF robot manipulator derived by using the Lagrangian method is formulated as below [27]:

$$\boldsymbol{H}(\boldsymbol{q})\ddot{\boldsymbol{q}} + \boldsymbol{C}(\boldsymbol{q},\dot{\boldsymbol{q}})\dot{\boldsymbol{q}} + \boldsymbol{G}(\boldsymbol{q}) = \boldsymbol{\tau} \tag{2}$$

where $q = [q_1 \quad q_2]$, $\tau = [\tau_1 \quad \tau_2]$, and

$$H = \begin{bmatrix} \alpha + 2\varepsilon cos(q_2) + 2\eta \sin(q_2) & \beta + \varepsilon cos(q_2) + \eta \sin(q_2) \\ \beta + \varepsilon cos(q_2) + \eta \sin(q_2) & \beta \end{bmatrix},$$
$$C = \begin{bmatrix} (-2\varepsilon sin(q_2) + 2\eta \cos(q_2))\dot{q}_2 & (-\varepsilon sin(q_2) + \eta \cos(q_2))\dot{q}_2 \\ (\varepsilon sin(q_2) - \eta \cos(q_2))\dot{q}_1 & 0 \end{bmatrix},$$
$$G = \begin{bmatrix} \varepsilon e_2 cos(q_1 + q_2) + \eta e_2 \sin(q_1 + q_2) + (\alpha - \beta + e_1)e_2 \cos(q_1) \\ \varepsilon e_2 cos(q_1 + q_2) + \eta e_2 \sin(q_1 + q_2) \end{bmatrix},$$

where $\alpha, \beta, \varepsilon$, and η are constant values calculated based on the manipulator parameters adopted from the data related to the human body, as given in Table 1 [28]. $\alpha = I_1 + m_1 l_{c1}^2 + I_e + m_e l_{ce}^2 + m_e l_1^2$, $\beta = I_e + m_e l_{ce}^2$, $\varepsilon = m_e l_1 l_{ce} \cos(\delta_e)$, $\eta = m_e l_1 l_{ce} \sin(\delta_e)$.

Table 1. Parameter values of a 2DOF revolute joint manipulator

m_1	l_1	l_{c1}	I_1	m_e	l_{ce}	I_e	δ_e	e_1	e_2
2.4 kg	0.3 m	0.15 m	$\frac{2.4}{12}$ kg.m^2	2 kg	0.5 m	$\frac{2}{12}$ kg.m^2	0	-0.408	$\frac{g}{0.3}$

$a = [\alpha \quad \beta \quad \varepsilon \quad \eta]^T$, and $\hat{a} = [\hat{\alpha} \quad \hat{\beta} \quad \hat{\varepsilon} \quad \hat{\eta}]^T$, where $\hat{a}$ is the estimation of a.

In this paper, $\tilde{a} = \hat{a} - a$ is assumed, and $\dot{\tilde{a}} = \dot{\hat{a}}$ because a is a vector of constant value. Matrices $\hat{H}, \hat{C}$, and $\hat{G}$ are the estimation of the matrices H, C, and G, respectively, and given as below:

$$\hat{H} = \begin{bmatrix} \hat{\alpha} + 2\hat{\varepsilon} cos(q_2) + 2\hat{\eta} \sin(q_2) & \hat{\beta} + \hat{\varepsilon} cos(q_2) + \hat{\eta} \sin(q_2) \\ \hat{\beta} + \hat{\varepsilon} cos(q_2) + \hat{\eta} \sin(q_2) & \hat{\beta} \end{bmatrix},$$

$$\hat{C} = \begin{bmatrix} (-2\hat{\varepsilon}sin(q_2) + 2\hat{\eta}\cos(q_2))\dot{q}_2 & (-\hat{\varepsilon}sin(q_2) + \hat{\eta}\cos(q_2))\dot{q}_2 \\ (\hat{\varepsilon}sin(q_2) - \hat{\eta}\cos(q_2))\dot{q}_1 & 0 \end{bmatrix}$$

$$\hat{G} = \begin{bmatrix} \hat{\varepsilon}e_2cos(q_1+q_2) + \hat{\eta}e_2\sin(q_1+q_2) + (\hat{\alpha} - \hat{\beta} + e_1)e_2\cos(q_1) \\ \hat{\varepsilon}e_2cos(q_1+q_2) + \hat{\eta}e_2\sin(q_1+q_2) \end{bmatrix}$$

3. SLIDING MODE CONTROL TECHNIQUE

The sliding mode has two essential, important phases. The first phase is the reaching phase, in which the system is derived to maintain a stable manifold. The second phase is the sliding phase, in which the system is derived and slides to equilibrium. Figure 2 represents the basic idea of the sliding mode (for more details about sliding mode, please see [29, 30]).

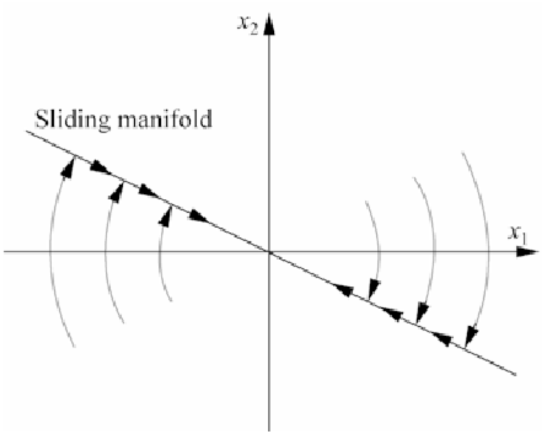

Figure 2. Basic principle of sliding mode [29]

3.1 Controlling According to the Stability of Input–Output

In this paper, the system is given in (2) with unknown constant parameters, and α, β, ε, and η are considered. The desired trajectory of the system is named q_d. Then, the tracking error is given by

$e = q_d - q,$
and
$\dot{q}_r = \dot{q}_d + \Lambda(q_d - q),$

where Λ is a diagonal positive matrix. Moreover, $p = a$, $\hat{p} = \hat{a}$, and $\tilde{p} = \tilde{a}$. Based on the linearity of the robotic characteristic [25], then

$$H(q)\ddot{q_r} + C(q,\dot{q})\dot{q_r} + G(q) = Y(q,\dot{q},\dot{q_r},\ddot{q_r})p \quad (3.a)$$
$$\tilde{H}(q)\ddot{q_r} + \tilde{C}(q,\dot{q})\dot{q_r} + \tilde{G}(q) = Y(q,\dot{q},\dot{q_r},\ddot{q_r})\tilde{p} \quad (3.b)$$

where $\tilde{H}(q) = H(q) - \hat{H}(q)$, $\tilde{C}(q,\dot{q}) = C(q,\dot{q}) - \hat{C}(q,\dot{q})$, $\tilde{G}(q) = G(q) - \hat{G}(q)$, and the dynamic regression matrix is given by

$$Y(q,\dot{q},\dot{q}_r,\ddot{q}_r) = \begin{bmatrix} Y_{11} & Y_{12} & Y_{13} & Y_{14} \\ Y_{21} & Y_{22} & Y_{23} & Y_{24} \end{bmatrix}, \quad (4)$$

where
$Y_{11} = \ddot{q}_{r1} + e_2\cos(q_1)$, $Y_{12} = \ddot{q}_{r2} - e_2\cos(q_1)$, $Y_{13} = 2\cos(q_2)\ddot{q}_{r1} + \cos(q_2)\ddot{q}_{r2} - 2\sin(q_2)\ \dot{q}_2\dot{q}_{r1} - \sin(q_2)\ \dot{q}_2\dot{q}_{r2} + e_2\cos(q_1+q_2)$, $Y_{14} = 2\sin(q_2)\ddot{q}_{r1} + \sin(q_2)\ddot{q}_{r2} + 2\cos(q_2)\ \dot{q}_2\dot{q}_{r1} + \cos(q_2)\ \dot{q}_2\dot{q}_{r2} + e_2\sin(q_1+q_2)$, $Y_{21} = 0$, $Y_{22} = \ddot{q}_{r1} + \ddot{q}_{r2}$, $Y_{23} = \cos(q_2)\ddot{q}_{r1} + \sin(q_2)\ \dot{q}_1\dot{q}_{r1} + e_2\cos(q_1+q_2)$, $Y_{24} = \sin(q_2)\ddot{q}_{r1} - \cos(q_2)\ \dot{q}_2\dot{q}_{r1} + e_2\sin(q_1+q_2)$.

To design a slide mode controller, the sliding variable and the Lyapunov function are selected as

$$s = \dot{s} + \Lambda e \quad (5)$$
$$V(t) = \frac{1}{2}\ s^T H(q)s$$

Therefore,

$$\dot{V}(t) = s^T H(q)\dot{s} + \frac{1}{2} s^T \dot{H}(q) s = s^T H(q)\dot{s} + s^T C(q,\dot{q}) s$$
$$= s^T [H(q)(\ddot{q}_r - \ddot{q}) + C(q,\dot{q})(\dot{q}_r - \dot{q})$$
$$= s^T [H(q)\ddot{q}_r + C(q,\dot{q})\dot{q}_r + G(q) - \tau] \quad (6)$$

The SMC can be realized by utilizing the following two approaches.

Approach 1: According to the estimated model

The design of the controller can be illustrated as

$$\tau = \hat{H}(q)\ddot{q}_r + \hat{C}(q,\dot{q})\dot{q}_r + \hat{G}(q) + \tau_s, \quad (7)$$

where τ_s represents the robustness element to be designed.

From Equations (6) and (7), the following equation can be found:

$$\dot{V}(t) = s^T [H(q)\ddot{q}_r + C(q,\dot{q})\dot{q}_r + G(q) - \hat{H}(q)\ddot{q}_r - \hat{C}(q,\dot{q})\dot{q}_r - \hat{G}(q) - \tau_s]$$
$$= s^T \left[\tilde{H}(q,\dot{q})\ddot{q}_r + \tilde{C}(q,\dot{q})\dot{q}_r + \tilde{G}(q) - \tau_s\right] = s^T [Y(q,\dot{q},\dot{q}_r,\ddot{q}_r)\tilde{p} - \tau_s],$$

Where,

$$\tilde{p} = [\tilde{p}_1 \ \ \tilde{p}_2 \ \ \tilde{p}_3 \ \ \tilde{p}_4]^T, \ |\tilde{p}_i| \le \bar{\tilde{p}}_i, \ i = 1,2,3,4$$
$$Y(q,\dot{q},\dot{q}_r,\ddot{q}_r) = [Y_{ij}], \ |Y_{ij}| \le \bar{Y}_{ij}, \ i = 1,2; \ j = 1,2,3,4$$

In this paper, robustness element, τ_s, is selected as

$$\tau_s = k_i \mathrm{sgn}(s) + s = \begin{bmatrix} k_1 \,\mathrm{sgn}(s_1) + s_1 \\ k_2 \,\mathrm{sgn}(s_2) + s_2 \end{bmatrix}, \quad (8)$$

where $k_i = \sum_{j=1}^{4} \bar{Y}_{ij} \bar{\tilde{p}}_i$, i=1,2.

Therefore, the following expression can be derived:

$$\dot{V}(t) = \sum_{i=1}^{2}\sum_{j=1}^{4} s_i Y_{ij} \ \tilde{p}_j - \sum_{i=1}^{2} s_i k_i \mathrm{sgn}(s_i) - \sum_{i=1}^{2} s_i^2$$
$$= \sum_{i=1}^{2}\sum_{j=1}^{4} s_i Y_{ij} \ \tilde{p}_j - \sum_{i=1}^{2} |s_i| \bar{Y}_{ij} \bar{\tilde{p}} \ - \sum_{i=1}^{2} s_i^2 \ \le \ -\sum_{i=1}^{2} s_i^2 \le 0$$

Approach 2: According to the bounded model

In this approach, Equation (6) can be formulated as

$$\dot{V} = -s^T [\tau - (H(q)\ddot{q}_r + C(q,\dot{q})\dot{q}_r + G(q))]$$
$$= -s^T [\tau - Y(q,\dot{q},\dot{q}_r,\ddot{q}_r)p]$$

The design of the controller becomes

$$\tau_s = \bar{k}_i \mathrm{sgn}(s) + s = \begin{bmatrix} \bar{k}_1 \,\mathrm{sgn}(s_1) + s_1 \\ \bar{k}_2 \,\mathrm{sgn}(s_2) + s_2 \end{bmatrix}, \quad (9)$$

where $\bar{k}_i = \sum_{j=1}^{4} \bar{Y}_{ij} \bar{p}_i$, i=1,2

Then, the following expression can be derived:

$$\dot{V}(t) = -\left[\sum_{i=1}^{2} s_i \bar{k}_i \mathrm{sgn}(s_i) + \sum_{i=1}^{2} s_i^2 - \sum_{i=1}^{2}\sum_{j=1}^{4} s_i Y_{ij}\ \bar{p}_j\right]$$

$$= -\left[\sum_{i=1}^{2}\sum_{j=1}^{4} |s_i| \bar{Y}_{ij}\ \bar{p}_j + \sum_{i=1}^{2} s_i^2 - \sum_{i=1}^{2} s_i Y_{ij} p_j\right] \le -\sum_{i=1}^{2} s_i^2 \le 0$$

According to the switching gain k_i of the controller given by Equation (8) and the switching gain $\bar{k}_i$ of the controller given by Equation (9), k_i is smaller than $\bar{k}_i$. Consequently, the controller that is given by Equation (7) produces chattering smaller than that produced by the controller given by Equation (9).

3.2 Controlling according to the adaptation algorithm

In this subsection, the slide mode controller is designed based on a simple computation adaptive control algorithm. The adaptation algorithm was presented by Slotine and Li [31].
With the same consideration that was presented in Subsection 3.1, the tracking error and its derivatives are given as

$$\tilde{q}(t) = q_d - q_d(t),$$
$$\dot{q}_r = \dot{q_d} - \Lambda\tilde{q},\ \ddot{q}_r = \ddot{q_d} - \Lambda\dot{\tilde{q}} \tag{10}$$

In this case, the sliding variable is defined as

$$s = \dot{\tilde{q}} + \Lambda\,\tilde{q} \tag{11}$$

The adaptive controller proposed by Soltine et al. [27] is given as

$$\tau = \hat{H}(q)\ddot{q}_r + \hat{C}(q,\dot{q})\dot{q}_r + \hat{G}(q) - K_D\, s, \tag{12}$$

where $K_D = \begin{bmatrix} k_{d1} & 0 \\ 0 & k_{d2} \end{bmatrix},\ k_{di} > 0,\ i = 1,2$

The Lyapunov function is selected according to the positive definite matrix H as

$$V(t) = \frac{1}{2}\, s^T H(q) s + \frac{1}{2}\, \tilde{a}^T \Gamma \tilde{a}$$

where $\Gamma = \begin{bmatrix} \gamma_1 & 0 & 0 & 0 \\ 0 & \gamma_2 & 0 & 0 \\ 0 & 0 & \gamma_3 & 0 \\ 0 & 0 & 0 & \gamma_4 \end{bmatrix}, \gamma_i > 0, i = 1,2,3,4$

Consequently, the following is obtained:

$$\dot{V}(t) = s^T H\dot{s} + \frac{1}{2}\, s^T \dot{H} s + \tilde{a}^T \Gamma \dot{\tilde{a}} = s^T(H\ddot{q} - H\ddot{q}_r) + \frac{1}{2} s^T \dot{H} s + \tilde{a}^T \Gamma \dot{\tilde{a}}$$
$$= s^T(\tau - +C\dot{q} - G - H\ddot{q}_r) + \frac{1}{2} s^T \dot{H} s + \tilde{a}^T \Gamma \dot{\tilde{a}}$$
$$= s^T(\tau - C(s + \dot{q}) - G - H\ddot{q}_r) + \frac{1}{2} s^T \dot{H} s + \tilde{a}^T \Gamma \dot{\tilde{a}}$$

By introducing τ from Equation (12), the following is obtained:

$$\dot{V} = s^T(\hat{H}\ddot{q}_r + \hat{C}\dot{q}_r + \hat{G} - K_D\, s - C(s + \dot{q}) - G - H\ddot{q}_r) + \frac{1}{2} s^T \dot{H} s + \tilde{a}^T \Gamma \dot{\tilde{a}}$$
$$= s^T(\tilde{H}\ddot{q}_r + \tilde{C}\dot{q}_r + \tilde{G} - K_D\, s - Cs) + \frac{1}{2} s^T \dot{H} s + \tilde{a}^T \Gamma \dot{\tilde{a}}$$

Moreover, based on the linearity of the robotic characteristic [1, 3–7, 10, 11] and the same as Equation (3b),

$$\tilde{H}\ddot{q_r} + \tilde{C}\dot{q}_r + \tilde{G} = Y(q,\dot{q},\dot{q}_r,\ddot{q}_r)\tilde{a} \quad (13)$$

Hence,

$$\dot{V} = s^T(Y\tilde{a} - K_D\, s - Cs) + \frac{1}{2}s^T\dot{H}s + \tilde{a}^T\Gamma\dot{\tilde{a}}$$
$$= s^T(Y\tilde{a} - K_D\, s) + \frac{1}{2}s^T(\dot{H} - 2C)s + \tilde{a}^T\Gamma\dot{\tilde{a}}$$
$$= s^T(Y\tilde{a} - K_D\, s) + \tilde{a}^T\Gamma\dot{\tilde{a}} = \tilde{a}^TY^T\, s - s^TK_Ds + \tilde{a}^T\Gamma\dot{\tilde{a}}$$
$$= \tilde{a}^T(Y^Ts + \Gamma\dot{\tilde{a}}) - s^TK_Ds$$

The rule of the adaptation was designed as follows [27, 31]:

$$\dot{\hat{a}} = -\Gamma^{-1}Y^Ts \quad (14)$$

Therefore,

$\dot{V}(t) = -s^TK_Ds \leq 0$, then $\tilde{q} \to 0$ as $t \to \infty$.

4. SIMULATION RESULTS

In this paper, the designed SMC is implemented by using the MATLAB platform by the m-files and the simulation options. For both controllers designed, the desired trajectories for the two joints of the robot arm are proposed as $q_{d1} = 2\cos\left(\frac{1}{2}\pi t\right)$ and $q_{d2} = 2\cos\left(\frac{1}{2}\pi t\right)$. The following manipulator parameters' constant values are calculated based on the data given in Table 1. The initial values of the positioning and velocity of the manipulator links are selected as $q_{io} = [1.5, 1, 1.5, 1]^T$ to be different from the desired values.

$$\alpha = 1.1, \quad \beta = 0.67, \quad \varepsilon = 0.3, \quad \eta = 0$$

4.1 SMC based on the stability of input–output

Figure 3 illustrates the Simulink construction for SMC based on the stability of the input–output controller SMCSIO. For this controller type, the controller parameters, Λ and $\hat{p}$, are selected after many tries, in which the best results are obtained:

$$\Lambda = \begin{bmatrix} 4.2 & 0 \\ 0 & 4.2 \end{bmatrix}, \hat{p} = 0.9p.$$

The SMC is attained by utilizing the first approach, in which the controller is given in Equation (7), where $\overline{p}_{\mathrm{i}} = |\tilde{p}_i| + 0.8$. The saturated function is adopted as a replacement for the switch function, where $\Delta = 0.04$. Figures 4–6 show the simulation responses for the proposed SMC. At the same time, identical simulation results are achieved when the second approach is utilized, in which the controller is given in Equation (9), where $\overline{p}_{\mathrm{i}} = |p_i| + 0.8$.

Figure 4 describes the behavior of both position and speed for joint 1 versus that of the desired position and speed. They need less than 0.8 s to coincide with the desired responses. Moreover, the position and the speed for joint 2 need less than 0.9 s to identify the desired responses, as shown in Figure 5. Figure 6 presents the control input responses for the two links according to the proposed controller.

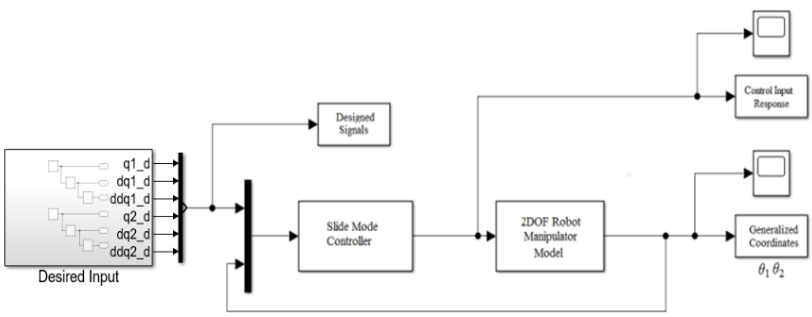

Figure 3. MATLAB simulation for SMC based on the stability of input–output controlling

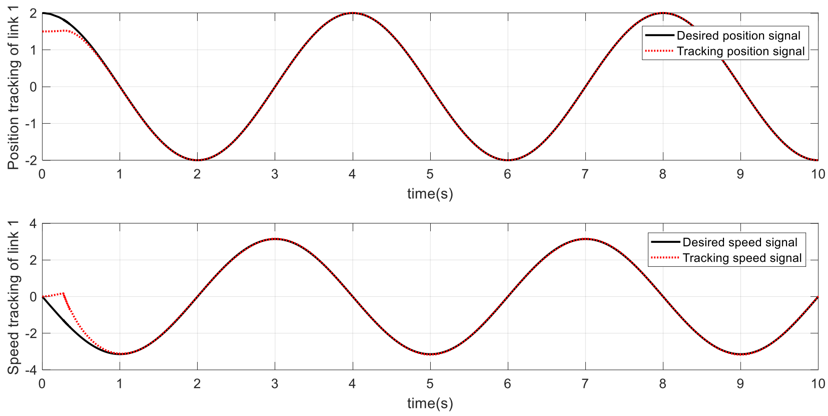

Figure 4. Positioning and speed tracking responses for the first link adopting SMCSIO

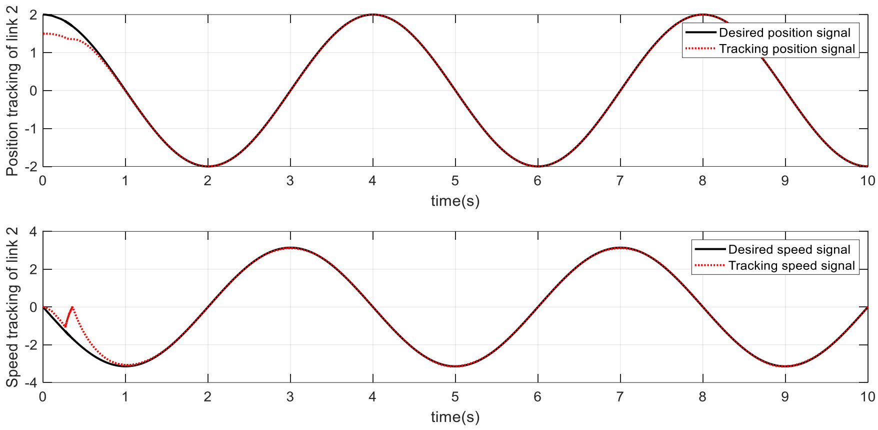

Figure 5. Positioning and speed tracking responses for the second link adopting SMCSIO

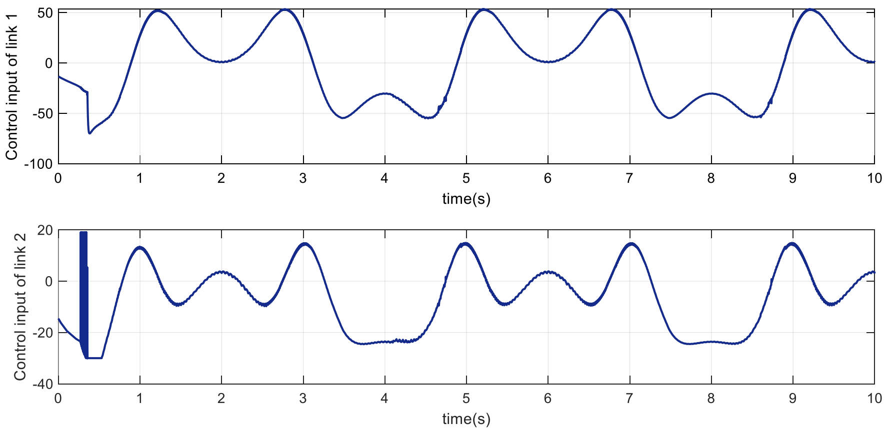

Figure 6 Control inputs responses for the two links for SMCSIO

4.2 SMC based on the adaptation

Figure 7 illustrates the Simulink construction for SMC based on the adaptation algorithm SMCA. The plant is considered as that given in Equation (3). Equations (12) and (14) are adopted for the controller and the adaptive rule, respectively. Moreover, the following controller parameters are selected after many tries, in which the combination of control action and the adaptation law provide the best results:

$\Lambda = \begin{bmatrix} 10 & 0 \\ 0 & 10 \end{bmatrix}$, $K_D = \begin{bmatrix} 50 & 0 \\ 0 & 50 \end{bmatrix}$, $\Gamma = \begin{bmatrix} 1.5 & 0 & 0 & 0 \\ 0 & 1.5 & 0 & 0 \\ 0 & 0 & 0.5 & 0 \\ 0 & 0 & 0 & 0.5 \end{bmatrix}$ and $Y(q, \dot{q}, \dot{q}_r, \ddot{q}_r)$ as given in Equation (4).

Figures 8–13 illustrate the output simulation responses of the currently proposed controller. Figures 8 and 9 show the position and speed trajectories of the two joints linked according to the desired input responses. The results explain the effectiveness of the proposed controller for both stability as well as the convergence of trajectory. The positing tracking error convergences for the two joints are presented in Figure 10. The controller is able to track the desired position very rapidly. Figure 11 illustrates the responses of the control inputs for the two links according to SMCA. Both control inputs do not differ so much from those obtained in Figure 6. This finding reveals the effectiveness of the proposed SMC for the two approaches.

In addition, Figures 12 and 13 provide the estimation parameters of the proposed SMC. The effects of recognition to constant values, α, β, ε, and η, are not satisfactory. Moreover, the adaptive law adopted in this paper ensures the convergence of the outputs with the desired responses. The most striking result to emerge from the data is that in the simulation of the adaptive control model, the error of the estimated parameter does not converge to 0 because tracking error convergence can be accomplished according to numerous probable values of the parameter estimated besides the true parameter. Consequently, the parameter adaptation law does not affect the operation of finding the true parameter [24].

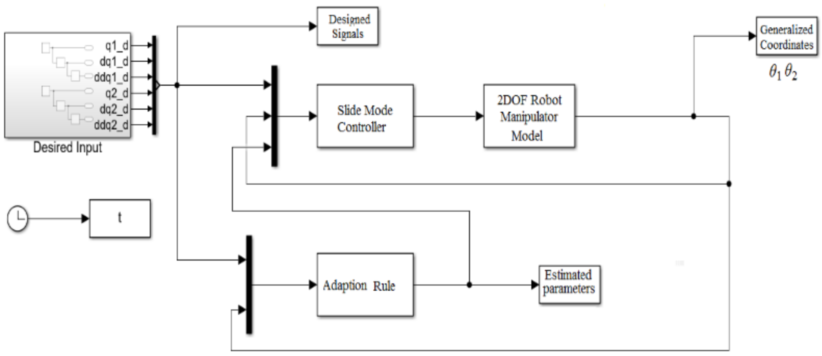

Figure 7. MATLAB simulation for SMC based on adaptation controlling

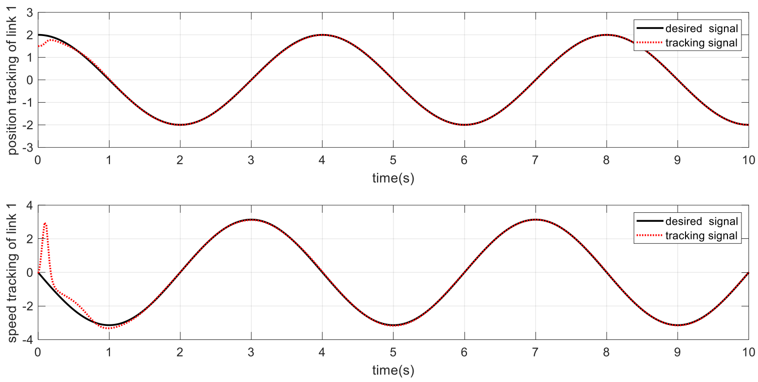

Figure 8. Positioning and speed tracking responses for the first link adopting SMCA

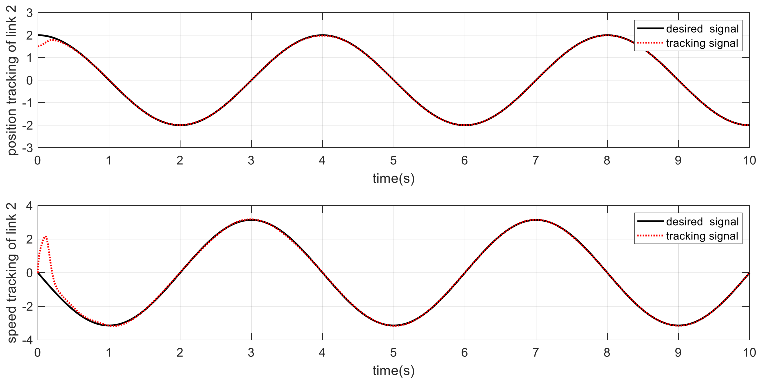

Figure 9. Positioning and speed tracking responses for the second link adopting SMCA

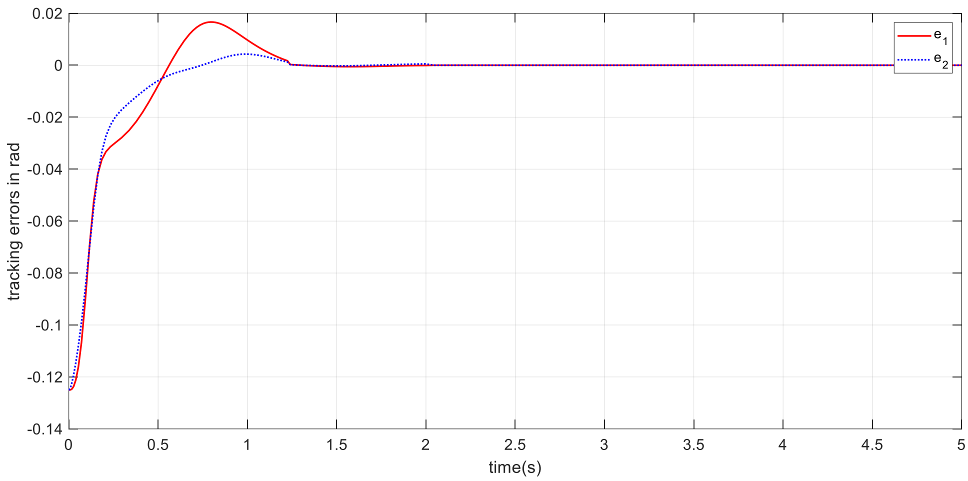

Figure 10. Tracking error responses of the two joints for SMCA

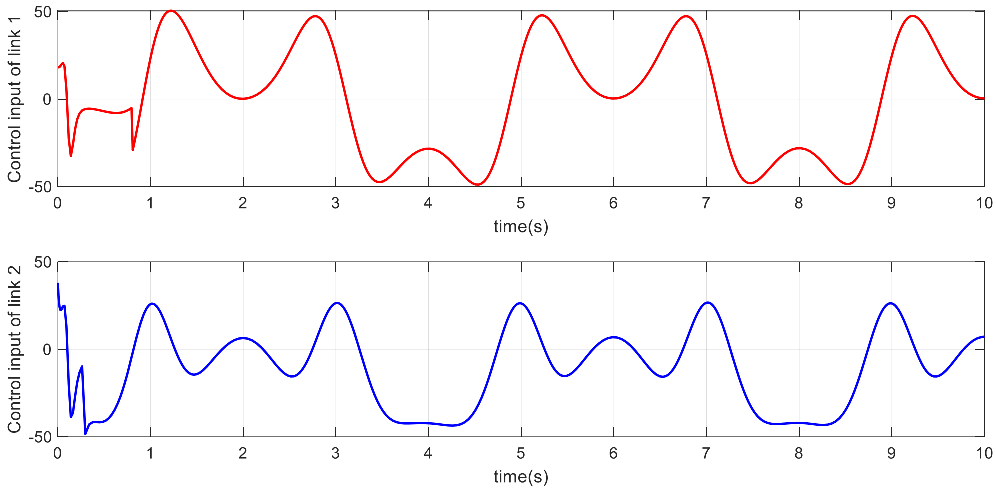

Figure 11. Control inputs responses for the two links for SMCA

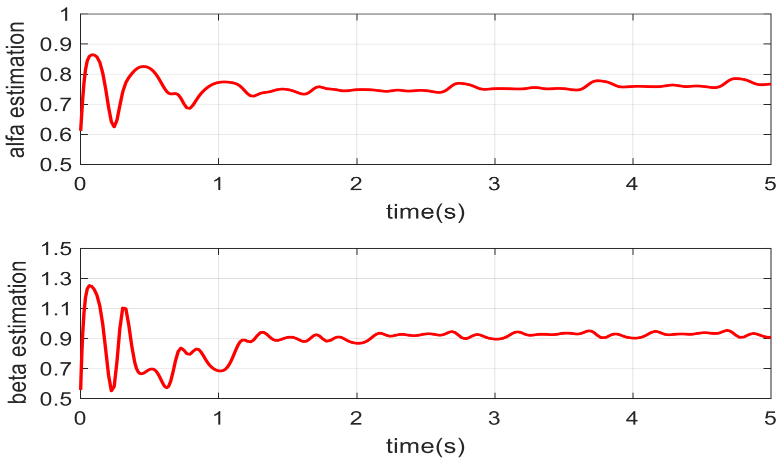

Figure 12. Estimated parameters α and β for SMCA

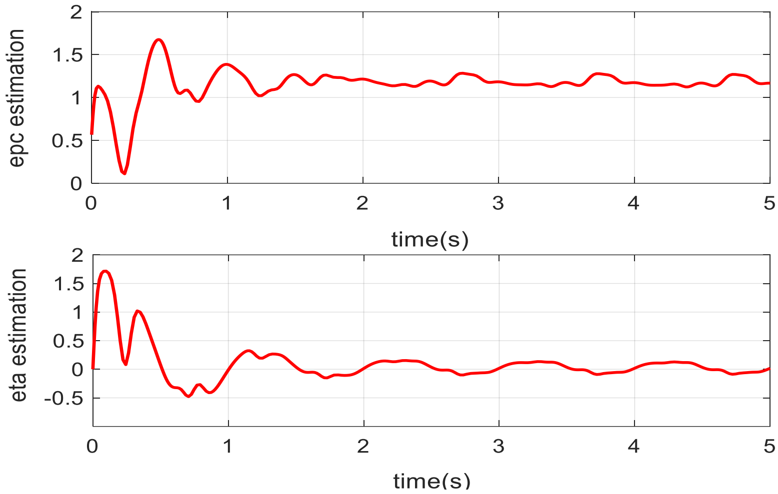

Figure 13. Estimated parameters ε and η for SMCA

5. DISCUSSION

SMC is well-known for its robustness to changes in system parameters and external disturbances, making it a highly desirable, cost-effective method for serial robots to execute high-precision control tasks. Kumar and colleagues developed an SMC for frequency regulation in an interconnected power system in 2021. For the LFC system model, they used four parameters. PSO and GWO techniques were used to acquire these parameters [20]. Wang et al. suggested a resilient, adaptable SMC subject to control input limits for both MIMO and SISO systems based on a finite time SMC technique [21]. The goal of this paper is to create a stable, reliable 2DOF robotic manipulator for the upper limb robotic model by the addition of adaptation law in the SMC scheme. Two SMCs are developed using the general manipulator equation of motion. The controllers' stability is assessed using Lyapunov stability criteria. The controllers and the robotic arm are formulated analytically.

According to the results obtained for the two proposed controllers, SMCSIO and SMCA, the tracking error responses of the manipulator's two joints show remarkable results, where the time required for zero error does not exceed 1 s for both schemes. Moreover, great stability is guaranteed based on the Lyapunov theorem. The results also show a remarkable minimization in the chattering of the output responses that is considered one of the drawbacks of the SMC technique. Moreover, the integral absolute error, $IAE = \int |e(t)|dt$, for the tracking error signal is calculated for both manipulator's joints according to SMC schemes SMCSIO and SMCA. This index is adopted to show the effectiveness of the SMCA compared with SMCSIO by calculating the improvement rate. Table 2 presents the IAE for the two joints. Despite the effectiveness of both controllers, the SMCA shows 40.5% and 36.7% tracking error response improvement rates of joints 1 and 2, respectively, compared with the tracking error achieved by SMCSIO.

Table 2. IAE index of tracking error for manipulator's joints

Joint Number	IAE index SMCSIO	IAE index SMCA	Improvement rate %
1	4.715	2.807	40.5
2	3.4976	2.213	36.7

6. CONCLUSIONS

In this paper, 2DOF serial link robot manipulator is studied and analyzed as a simple robotic arm used in medical applications. The main contribution of is the addition of adaptation law in the SMC scheme to improve the tracking accuracy and stability of the 2DOF manipulator robot. Based on the dynamic equation of the manipulators, two different types of SMC control techniques are proposed. The input–output stability and adaptation sliding mode controllers for the 2DOF robotic arm are designed according to the stability properties of the system, ensuring that the adaptive gain of the controller meets the Lyapunov stability theorem requirements. The controllers are proven analytically and confirmed by a MATLAB simulation. According to the results obtained, the following are concluded:

i. Remarkable positioning and speed trajectory tracking are achieved for both links joints 1 and 2.
ii. High-stability responses based on Lyapunov stability theorem are obtained.
iii. Although the estimated parameters in the adaptation SMC do not converge to 0, the adaptation law highly approaches the true parameters.
iv. The SMC design is more appropriate for the robotic arm plant because of its ability of disturbance rejection, lower chattering, and smaller tracking error.

The proposed model could be performed practically for future research by tuning the adaptation controller parameters using optimization methods such as PSO, GWO, Artificial Bee Colony (ABC), Fish School Search (FSS).

Conflict of interest
The authors declare no conflict of interest.

Compliance with ethical standards
Ethical approval: This article does not contain any study with human participants or animals performed by the authors.

Financial Support:
Not applicable.

REFERENCES
[1] A. Frisoli *et al.*, "Positive effects of robotic exoskeleton training of upper limb reaching movements after stroke," *Journal of NeuroEngineering and Rehabilitation*, vol. 9, no. 1, pp. 1–16, Jun. 2012, doi: 10.1186/1743-0003-9-36/FIGURES/13.
[2] H. K. Aljobouri, "A Virtual EMG Signal Control and Analysis for Optimal Hardware Design," *International Journal of Online and Biomedical Engineering (iJOE)*, vol. 18, no. 02, pp. 154–166, Feb. 2022, doi: 10.3991/IJOE.V18I02.27047.
[3] Y.-H. Kim, "Robotic assisted rehabilitation therapy for enhancing gait and motor function after stroke," *Precision and Future Medicine*, vol. 3, no. 3, pp. 103–115, Sep. 2019, doi: 10.23838/PFM.2019.00065.
[4] S. Taravati, K. Capaci, H. Uzumcugil, and G. Tanigor, "Evaluation of an upper limb robotic rehabilitation program on motor functions, quality of life, cognition, and emotional status in patients with stroke: a randomized controlled study," *Neurological sciences : official journal of the Italian Neurological Society and of the Italian Society of Clinical Neurophysiology*, vol. 43, no. 2, pp. 1177–1188, Feb. 2022, doi: 10.1007/S10072-021-05431-8.
[5] T. A. Mai and T. S. Dang, "Optimal fuzzy PD control for a two-link robot manipulator based on stochastic fractal search," *The European Physical Journal Special Topics 2021 230:21*, vol. 230, no. 21, pp. 3935–3945, Nov. 2021, doi: 10.1140/EPJS/S11734-021-00339-Y.
[6] M. U. Khan and T. Kara, "Adaptive Control of a Two-Link Flexible Manipulator Using a Type-2 Neural Fuzzy System," *Arabian Journal for Science and Engineering*, vol. 45, no. 3, pp. 1949–1960, Mar. 2020, doi: 10.1007/S13369-020-04341-9.
[7] K. Jayaswal, D. K. Palwalia, and S. Kumar, "Performance investigation of PID controller in trajectory control of two-link robotic manipulator in medical robots," *https://doi.org/10.1080/09720502.2021.1893444*, vol. 24, no. 2, pp. 467–478, 2021, doi: 10.1080/09720502.2021.1893444.
[8] S. Mikha, H. K. Aljobouri, and A. affiliations, "CPAP Hardware/Simulation and Control Design for Respiratory Disorders: A Review," *Al-Nahrain Journal for Engineering Sciences*, vol. 24, no. 2, pp. 112–122, Dec. 2021, doi: 10.29194/NJES.24020112.
[9] A. sabeeh Mikha and H. K. Aljobouri, "Simulation of continuous positive airway pressure device equipped with BLDC motor," *AIP Conference Proceedings*, vol. 2386, no. 1, p. 040007, Jan. 2022, doi: 10.1063/5.0066880.
[10] B. Mahboub and D. Stephen, "A Two-Link Robot Manipulator: Simulation and Control Design," *International Journal of Robotic Engineering*, vol. 5, no. 2, Dec. 2020, doi: 10.35840/2631-5106/4128.
[11] S. Ilgen, A. Durdu, E. Gulbahce, and A. Cakan, "Optimal Tuning of the SMC Parameters for a Two-Link Manipulator Co-Simulation Control," *Elektronika ir Elektrotechnika*, vol. 27, no. 5, pp. 4–10, Oct. 2021, doi: 10.5755/J02.EIE.28954.
[12] R. P. Mathew and A. Sareena, "Application of PID Controller and Nonlinear Sliding Mode Control on Two Link Robotic Manipulator," *International Journal of Engineering Research & Technology*, vol. 8, no. 5, 2019, Accessed: Apr. 28, 2022. [Online]. Available: www.ijert.org
[13] Zulfatman, M. Marzuki, N. Alif Mardiyah, Zulfatman, M. Marzuki, and N. Alif Mardiyah, "Two-Link Flexible Manipulator Control Using Sliding Mode Control Based Linear Matrix Inequality," *MS&E*, vol. 190, no. 1, p. 012008, 2017, doi: 10.1088/1757-899X/190/1/012008.
[14] J. Li, Y. Wang, Z. Liu, X. Jing, and C. Hu, "A New Recursive Composite Adaptive Controller for Robot Manipulators," *Space: Science & Technology*, vol. 2021, pp. 1–7, Oct. 2021, doi: 10.34133/2021/9801421.

[15] B. Zhan, M. Jin, and J. Liu, "Extended-state-observer-based adaptive control of flexible-joint space manipulators with system uncertainties," *Advances in Space Research*, vol. 69, no. 8, pp. 3088–3102, Apr. 2022, doi: 10.1016/J.ASR.2022.01.016.

[16] S. M. Haris and W. S. Aboud, "Multiple model adaptive control of a nonlinear active vehicle suspension," in *International Conference on Advanced Mechatronic Systems, ICAMechS*, Jul. 2016, vol. 0, pp. 153–158. doi: 10.1109/ICAMECHS.2016.7813438.

[17] A. Liu, H. Zhao, T. Song, Z. Liu, H. Wang, and D. Sun, "Adaptive control of manipulator based on neural network," *Neural Computing and Applications 2020 33:9*, vol. 33, no. 9, pp. 4077–4085, Nov. 2020, doi: 10.1007/S00521-020-05515-0.

[18] X. Yin, L. Pan, and S. Cai, "Robust adaptive fuzzy sliding mode trajectory tracking control for serial robotic manipulators," *Robotics and Computer-Integrated Manufacturing*, vol. 72, p. 101884, Dec. 2021, doi: 10.1016/J.RCIM.2019.101884.

[19] M. Mucientes and J. Casillas, "Quick design of fuzzy controllers with good interpretability in mobile robotics," *IEEE Transactions on Fuzzy Systems*, vol. 15, no. 4, pp. 636–651, Aug. 2007, doi: 10.1109/TFUZZ.2006.889889.

[20] A. Kumar, M. N. Anwar, and S. Kumar, "Sliding mode controller design for frequency regulation in an interconnected power system," *Protection and Control of Modern Power Systems*, vol. 6, no. 1, pp. 1–12, Dec. 2021, doi: 10.1186/S41601-021-00183-1/FIGURES/27.

[21] B. Wang *et al.*, "Experimental validation of disturbance observer-based adaptive terminal sliding mode control subject to control input limitations for SISO and MIMO systems," *European Journal of Control*, vol. 63, pp. 151–163, Jan. 2022, doi: 10.1016/J.EJCON.2021.09.010.

[22] A. A. Khalate, G. Leena, G. Ray, A. A. Khalate, G. Leena, and G. Ray, "An Adaptive Fuzzy Controller for Trajectory Tracking of Robot Manipulator," *Intelligent Control and Automation*, vol. 2, no. 4, pp. 364–370, Oct. 2011, doi: 10.4236/ICA.2011.24041.

[23] M. W. Spong and M. Vidyasagar, *Robot Dynamics and Control | Wiley*. 2004. Accessed: Apr. 28, 2022. [Online]. Available: https://www.wiley.com/en-us/Robot+Dynamics+and+Control-p-9780471612438

[24] Y. Xia, W. Xie, J. Ma, and S. Su, "Research on trajectory tracking control of manipulator based on modified terminal sliding mode with double power reaching law," *Advanced Control for Robotics and Autonomous Systems*, vol. 16, no. 3, pp. 1–10, 2019, doi: 10.1177/1729881419847899.

[25] S. Kawamura and M. Svinin, *Advances in robot control: From everyday physics to human-like movements*. Springer Berlin Heidelberg, 2006. doi: 10.1007/978-3-540-37347-6.

[26] M. Trojanová, T. Čakurda, A. Hošovský, and T. Krenický, "Estimation of Grey-Box Dynamic Model of 2-DOF Pneumatic Actuator Robotic Arm Using Gravity Tests," *Applied Sciences 2021, Vol. 11, Page 4490*, vol. 11, no. 10, p. 4490, May 2021, doi: 10.3390/APP11104490.

[27] J.-J. E. Slotine and W. Li, *APPLIED NONLINEAR CONTROL*. 1991.

[28] R. H. Krishnan, V. Devanandh, A. K. Brahma, and S. Pugazhenthi, "ESTIMATION OF MASS MOMENT OF INERTIA OF HUMAN BODY, WHEN BENDING FORWARD, FOR THE DESIGN OF A SELF-TRANSFER ROBOTIC FACILITY," *Journal of Engineering Science and Technology*, vol. 11, no. 2, pp. 166–176, 2016.

[29] A. T. Azar and Q. Zhu, *Advances and applications in sliding mode control systems*, vol. 576. Springer Verlag, 2015. doi: 10.1007/978-3-319-11173-5.

[30] S. Vaidyanathan and C. H. Lien, *Applications of sliding mode control in science and engineering*, vol. 709. Springer Verlag, 2017. doi: 10.1007/978-3-319-55598-0.

[31] J. J. E. Slotine and W. Li, "On the Adaptive Control of Robot Manipulators:," *The International Journal of Robotics Research*, vol. 6, no. 3, pp. 49–59, Jul. 1987, doi: 10.1177/027836498700600303.